US Army Corps
of Engineers

STRENGTH PROPERTY ESTIMATION FOR DRY, COHESIONLESS SOILS USING THE MILITARY CONE PENETROMETER

by

William E. Perkins

Department of Civil and Mechanical Engineering
United States Military Academy
West Point, New York   10996

and

Roger W. Meier, John V. Farr

Geotechnical Laboratory

DEPARTMENT OF THE ARMY
Waterways Experiment Station, Corps of Engineers
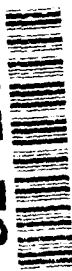3909 Halls Ferry Road, Vicksburg, Mississippi   39180-6199

May 1992
Final Report

GEOTECHNICAL LABORATORY

92-24831

92 9 08 024

REPORT DOCUMENTATION PAGE		Form Approved OMB No. 0704-0188

Public reporting burden for this collection of information is estimated to average 1 hour per response, including the time for reviewing instructions, searching existing data sources, gathering and maintaining the data needed, and completing and reviewing the collection of information. Send comments regarding this burden estimate or any other aspect of this collection of information, including suggestions for reducing this burden, to Washington Headquarters Services, Directorate for Information Operations and Reports, 1215 Jefferson Davis Highway, Suite 1204, Arlington, VA 22202-4302, and to the Office of Management and Budget, Paperwork Reduction Project (0704-0188), Washington, DC 20503.

1. AGENCY USE ONLY (Leave blank)	2. REPORT DATE May 1992	3. REPORT TYPE AND DATES COVERED Final report

4. TITLE AND SUBTITLE	5. FUNDING NUMBERS
Strength Property Estimation for Dry, Cohesionless Soils Using the Military Cone Penetrometer	DA Project AT40-AM-007

6. AUTHOR(S)

William E. Perkins, Roger W. Meier, John V. Farr

7. PERFORMING ORGANIZATION NAME(S) AND ADDRESS(ES)	8. PERFORMING ORGANIZATION REPORT NUMBER
USAE Waterways Experiment Station Geotechnical Laboratory, 3909 Halls Ferry Road Vicksburg, MS 39180-6199	Technical Report GL-92-5

9. SPONSORING/MONITORING AGENCY NAME(S) AND ADDRESS(ES)	10. SPONSORING/MONITORING AGENCY REPORT NUMBER
US Army Corps of Engineers Washington, DC 20314-1000	

11. SUPPLEMENTARY NOTES

Available from National Technical Service, 5285 Port Royal Road, Springfield, VA 22161

12a. DISTRIBUTION/AVAILABILITY STATEMENT	12b. DISTRIBUTION CODE
Approved for public release; distribution is unlimited.	

13. ABSTRACT (Maximum 200 words)

The US Army Engineer Waterways Experiment Station (WES) has successfully used cone index (CI) values obtained from the Military Cone Penetrometer Test to characterize soil strength since the 1950's. Over the past 40 years, WES has accumulated a large database of CI values throughout the world. These CI values have been used in empirical vehicle-soil interaction relationships to predict vehicle performance. These empirical relationships are rapidly being replaced by more theoretical models that rely on Newtonian physics and complicated track-soil and tire-soil interaction models to predict vehicle performance. The newer, more theoretical models require that the soil be characterized by funda-mental engineering properties such as friction angle, shear modulus, and unit weight rather than simple index properties. In order to make use of existing and future bodies of CI data worldwide, relationships must be developed for translating CI values into fundamental engineering properties. As a starting

(Continued)

14. SUBJECT TERMS		15. NUMBER OF PAGES 55
Cavity expansion Mobility Cone index Soil strength Cone penetrometer Surfical soils		
		16. PRICE CODE

17. SECURITY CLASSIFICATION OF REPORT	18. SECURITY CLASSIFICATION OF THIS PAGE	19. SECURITY CLASSIFICATION OF ABSTRACT	20. LIMITATION OF ABSTRACT
Unclassified	Unclassified		

13. ASTRACT (Concluded).

point, a simple system has been developed for estimating the unit weight, friction angle, and shear modulus of dry, cohesionless soils based solely on their Unified Soil Classification System soil classification and CI values obtained in the field. That system is detailed in this report and a limited amount of available validation data is presented.

PREFACE

The work described herein was conducted by personnel of the Department of Civil and Mechanical Engineering, US Military Academy (USMA), West Point, New York, and the Combat Engineering and Simulations Group (CESG), Modeling and Methodology Branch (MMB), Mobility Systems Division (MSD), Geotechnical Laboratory (GL), US Army Engineer Waterways Experiment Station (WES), Vicksburg, Mississippi. The work was sponsored by Headquarters, US Army Corps of Engineers, and was part of DA Project AT40-AM-007, under "Inference of Classical Soil Mechanics Properties." This work was conducted between 1 June 1991 and 31 December 1991.

The analytical work was performed by and the report was written by MAJ William E. Perkins, USMA; Mr. Roger W. Meier, CESG, GL; and Dr. John V. Farr, CESG, GL. The study was conducted under the direct supervision of Dr. Farr, Team Leader, under the general direction of Mr. Donald Randolph, Chief, MMB; Mr. Newell Murphy, Jr., Chief, MSD, GL; and Dr. William F. Marcuson III, Director, GL.

At the time of publication of this report, Director of WES was Dr. Robert W. Whalin. Commander and Deputy Director was COL Leonard G. Hassell, EN.

1

CONTENTS

LIST OF TABLES

LIST OF FIGURES

CONVERSION FACTORS, NON-SI TO SI (METRIC)
UNITS OF MEASUREMENT

Non-SI units of measurement used in this report can be converted to SI
(metric) units as follows:

Multiply	By	To Obtain
degrees (angle)	0.01745329	radians
inches	2.54	centimetres
miles (US statute)	1.609347	kilometres
pounds (force)	4.448222	newtons
pounds (force) per square inch	6.894757	kilopascals
pounds (mass) per cubic foot	16.01846	kilograms per cubic metre
pounds (mass) per cubic inch	27.6799	grams per cubic centimetre
square inches	6.4516	square centimetres

STRENGTH PROPERTY ESTIMATION FOR DRY, COHESIONLESS
SOILS USING THE MILITARY CONE PENETROMETER

PART I: INTRODUCTION

Background

1. The US Army Engineer Waterways Experiment Station (WES) has success-fully used cone index (CI) values obtained from the Military Cone Penetrometer Test (MCPT) (see Figure 1) to characterize soil strength since the 1950's. Over the ensuing 40 years, WES accumulated a large database of CI values from around the world. These CI values are used in empirical vehicle-soil interaction relationships to predict vehicle performance (Rula and Nutall 1971). The empirical relationships have been developed and refined based on extensive field testing of tracked and wheeled vehicles. However, these empirical rela-tionships are limited in their ability to model the detailed physics of vehicle-soil interaction required for describing the performance of
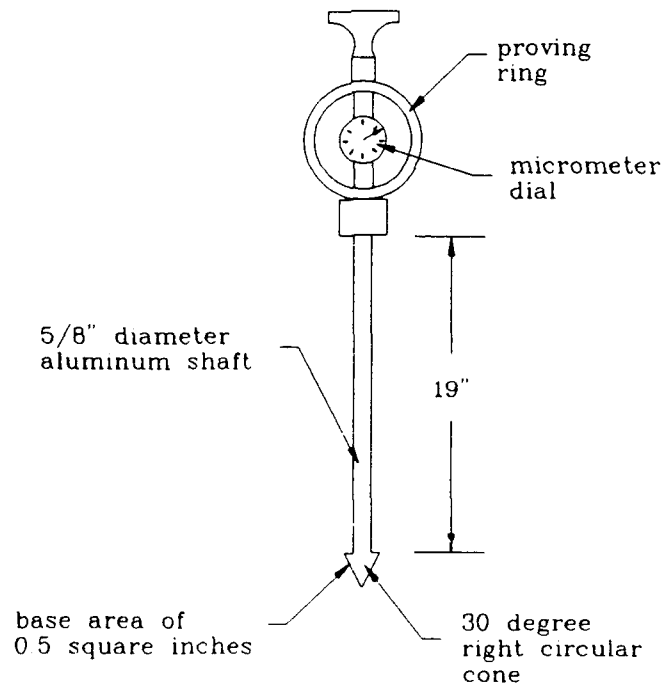
Figure 1. Standard military cone penetrometer

maneuvering vehicles, the deformation and compaction of soils resulting from traffic, and next-generation vehicles whose characteristics fall outside the range of the empirical relations. To address this problem, vehicle-terrain interaction models have become increasingly theoretical, relying on Newtonian physics and complicated track-soil and tire-soil interaction models to predict vehicle performance. The newer, more theoretical models require that the soil be characterized by fundamental engineering properties such as cohesion, friction angle, shear modulus, and unit weight rather than simple index properties such as CI.

2. The required soil properties could be obtained directly from a triaxial shear or direct shear test; however, tests such as those are expensive and time-consuming and could not begin to replace the existing body of accumulated CI data. The MCPT, on the other hand, is a simple, easy-to-operate, man-portable device that provides a rapid and inexpensive means of indirectly gaging soil strength in the field. Unfortunately, the MCPT only provides an indirect measure of soil strength (the index property C_i) rather than a direct measure of strength and deformation. In order to make use of both the existing and future bodies of CI data worldwide, correlations with which we can infer engineering properties from CI measurements must be developed.

3. A first attempt at inferring engineering properties from MCPT data was undertaken by Meier and Baladi (1988). Their methodology is based on a theoretical formulation of the CI problem using cavity expansion theory to relate cone penetration resistance to the strength and deformation properties of the soil. The cavity expansion formulation, originally derived by Rohani and Baladi (1981), incorporates three mechanical properties (cohesion, friction angle, and shear modulus) and the total unit weight. Obviously, these four unknown soil properties cannot be back-calculated directly from a single CI measurement. To ameliorate this problem, Meier and Baladi estimate the total unit weight and shear modulus of the soil based on its Unified Soil Classification System (USCS) soil classification, then calculate cohesion and friction angle from two CI measurements taken at different depths. This is accomplished by simultaneously solving two cavity expansion equations (one at each depth) for the two remaining unknowns.

4. The biggest drawback to the Meier and Baladi approach is that it assumes the material is homogeneous between the two measurement depths. The

6

methodology works fairly well for granular materials because they are reasonably homogeneous across short distances. The properties calculated for cohesive materials, however, are not always representative of the actual *in situ* soil strength because the *in situ* strength varies with depth due to changes in parameters such as stress history, water content, and root density.

5. Farr (1991) eliminated the need for two CI measurements at different depths by estimating three of the four unknowns (shear modulus, unit weight, and friction angle) based on the USCS soil classification and solving for the remaining unknown (cohesion) using the measured CI. The drawback to this approach is that it does not make full use of the measured CI in cohesionless soils. Because the cohesion is not actually an unknown--it is supposed to be either identically zero or very nearly zero--there is no need to solve for it using the measured CI. The measured CI is merely used to confirm that the three estimated soil properties (friction angle, shear modulus, and unit weight) are consistent with a soil having little or no cohesion. This deficiency is addressed by the work presented here.

Purpose

6. This report describes the development of a simple methodology for estimating the unit weight, friction angle, and elastic shear modulus of dry, cohesionless soils based solely on their classification within the USCS and CI values obtained from the field. The methodology is based on a cavity expansion formulation of the cone penetration problem and empirical correlations between the mechanical and physical properties of soils.

Scope

7. Part II presents an overview of the theoretical basis for the proposed methodology. Part III details the algorithms used to estimate the mechanical properties of soils using CI and soil classification. Part IV presents a partial validation of the methodology which is limited by the availability of suitable validation data. Part V contains a summary and the conclusions.

8. This report also contains four appendixes. Appendix A enumerates the soil designations used in the USCS. Appendix B presents the mathematical derivation of the cavity expansion theory upon which the methodology is based. Appendix C contains a listing of a FORTRAN subroutine implementing the methodology. Appendix D contains a listing of the notation used in this report.

PART II: THEORETICAL FORMULATION OF CONE INDEX

Background

9.   There are many correlations between cone penetration resistance and soil strength available for use in analyzing foundation engineering problems. Unfortunately, very little research has been directed toward the more complex problem of characterizing the surficial soils (i.e., to depths of 1 or 2 ft*) that are of interest in mobility applications. Karafiath and Nowatzki (1978) present a solution for the penetration resistance of surficial soils based on plasticity theory. Their formulation is useful for investigating the effects of cone geometry and penetration depth, but plasticity theory does not take the stiffness characteristics of the soil into account. It is well known that soil compressibility substantially affects penetration resistance (e.g., Vesić 1963; Robertson and Campanella 1983), so their approach is not particularly well suited to investigating the influence of soil properties on penetration resistance.

10.   Rohani and Baladi (1981) used the cavity expansion theory developed by Vesić (1972) in their formulation of cone penetration resistance. Cavity expansion theory has been used extensively for describing cone penetration and pile penetration resistance at depth (e.g., Baligh 1976; Vesić 1977; Baldi et al., 1981; Greeuw et al. 1988) because it takes both the strength and the stiffness of the soil into account. Stiffness is a particularly important consideration in the penetration of surficial soils because the soil is not vertically constrained and will be displaced around the cone and toward the ground surface, thus lessening its apparent stiffness. Because it takes stiffness into account, cavity expansion theory has been adopted as the basis of the methodology described here.

---

* A table of factors for converting non-SI to SI (metric) units of measurement is presented on page 4.

Formulation of the Problem

11. The standard military cone penetrometer consists of a proving ring, a micrometer dial, and a 30-degree right circular cone with a base area of 0.5 in.^{2} connected to an aluminum staff (see Figure 1). While the cone is advanced into the soil by hand at a more-or-less constant rate, the micrometer dial is read, usually at 1-in. penetration intervals, to obtain the penetration resistance. The micrometer dial is calibrated to read the CI directly. (The simplicity of the test is self-evident!)

12. The CI is actually derived from the vertical force F_z acting on the cone tip as

$$CI = \frac{4 F_z}{\pi D^2} \tag{1}$$

where D is the diameter of the cone tip. This equation converts the measured force to an index value having units of stress.

13. The basic geometry of the cone tip is shown in Figure 2. The cone tip can be characterized by its base diameter D , length L , and apex angle 2α (which are, of course, related through $L \tan \alpha = D/2$). For the standard WES mobility cone, L = 1.48 in., D = 0.799 in., and 2α = 30 degrees. A smaller version of the cone is also available and is often used in particularly strong soils that would be difficult to penetrate by hand with the larger cone. For the smaller cone tip, L = 0.93 in. and D = 0.5 in., thus the base area is 0.2 in.^{2} instead of 0.5 in.^{2}.

Stresses Resisting Cone Motion

14. If the tip of the cone is located at a distance Z+L from the ground surface, the stresses acting on a finite frustrum of the cone at a depth $Z+L-\eta$ are shown in Figure 2b. In that figure, σ and τ are the normal and shearing stresses, respectively, that are resisting penetration of the cone. Integration of these stresses over the surface of the cone will provide the magnitude of the vertical force F_z :

10

$$F_z = \int_0^L (\sigma \tan\alpha + \tau)\, 2\pi r\, d\eta \tag{2}$$

where $r = \eta \tan \alpha$. The stresses σ and τ are not known *a priori*, so they must be determined from the fundamental properties of the soil.

15. It has been observed in practice that the cone tends to shear the surrounding material during penetration and the soil is observed to flow around the cone tip and towards the surface. This indicates that the entire shearing strength of the soil is being mobilized, so the normal and shearing stresses in the soil can be related through some type of failure relationship.
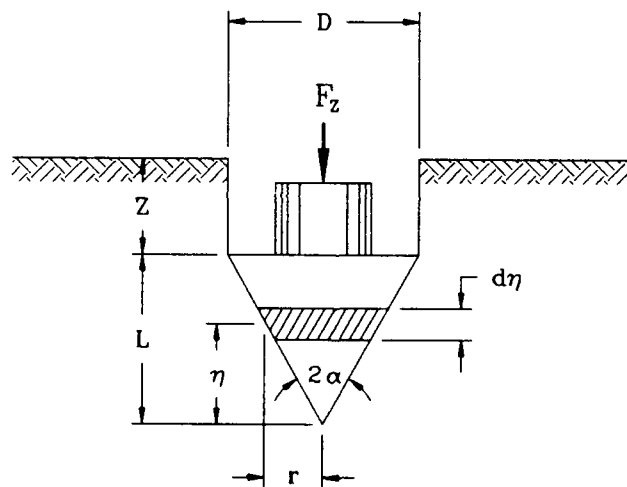
a. Geometry of the problem.
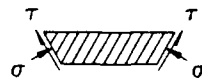
b. Stresses on a finite frustrum of the cone

Figure 2. The cone penetration problem

11

Assuming a Mohr-Coulomb failure criterion, the normal and shearing stresses are related as:

$$\tau = c + \sigma \tan\phi \qquad (3)$$

where c is the Mohr-Coulomb cohesion intercept and ϕ is the Mohr-Coulomb friction angle.

16. To determine the magnitude of the normal stress σ acting on the cone, the penetration of the cone can be equated to the expansion of a series of spherical cavities and the normal stress computed as the internal pressure needed to maintain a slow expansion of those cavities. Vesić (1972) was the first to solve the cavity expansion problem for materials possessing both cohesion and friction. His solution is summarized in Appendix B.

17. For soils having both cohesive and frictional strength components (i.e., c > 0 and tan ϕ > 0), the internal pressure needed to maintain a steady expansion of a spherical cavity can be expressed as:

$$\sigma = 3(q + c \cot\phi)\left(\frac{1 + \sin\phi}{3 - \sin\phi}\right) I_{rr}^m - c \cot\phi \qquad (4)$$

(from Appendix B) where q is the ambient hydrostatic stress existing prior to the application of the stresses at the cavity surface,

$$m = \frac{4 \sin\phi}{3(1 + \sin\phi)}$$

$$I_{rr} = \frac{I_r}{1 + \Delta I_r}$$

$$I_r = \frac{G}{c + q \tan\phi}$$

and G is the elastic shear modulus.

12

18. Referring back to the analogue of a series of expanding spherical cavities, the hydrostatic stress applicable to each of those cavities can be defined by $q = \gamma z$, where γ is the total unit weight of the soil and z is the depth below the ground surface. The *in situ* stress corresponding to a depth of $Z+L-\eta$ (Figure 2a) is therefore given by

$$q = (Z + L - \eta)\, \gamma \qquad (5)$$

As the stresses are integrated down the length of the cone, this equation can be used to obtain the field stresses surrounding the corresponding cavities.

Calculating the Cone Index

19. Combining Equations 1 through 5 and completing the integration for F_z , the following expression for CI is obtained:

$$CI = 6\, G^m \left(\frac{1 + \sin\phi}{3 - \sin\phi} \right) \left(\frac{\tan\alpha + \tan\phi}{\tan\alpha \cdot \tan\phi} \right) \Omega - c \cot\phi \qquad (6)$$

where

$$\Omega = \frac{[C + (Z+L)\,\gamma \tan\phi]^{3-m} - [C + (Z+L)\,\gamma \tan\phi + (2-m)\, L\gamma \tan\phi]\,(C + Z\gamma \tan\phi)^{2-m}}{(2-m)\,(3-m)\,(L\gamma \tan\phi)^2}$$

20. For the granular soils of interest here, the cohesion intercept is zero and the expression above simplifies to

$$CI = 6\, G^m \left(\frac{1 + \sin\phi}{3 - \sin\phi} \right) \left(\frac{\tan\alpha + \tan\phi}{\tan\alpha \cdot \tan\phi} \right) \Omega \qquad (7)$$

13

where

$$\Omega = \frac{[(Z+L)\gamma\tan\phi]^{3-m} - [Z\gamma\tan\phi + (3-m)L\gamma\tan\phi](Z\gamma\tan\phi)^{2-m}}{(2-m)(3-m)(L\gamma\tan\phi)^2}$$

21.   Equation 7 expresses the CI in terms of the fundamental soil prop-
erties ϕ , G , and γ plus the depth and geometry of the cone.   Our goal of
relating CI measurements to fundamental soil properties has been met; however,
we are still faced with the problem of having a single equation with three
unknowns.   The problem can only be made tractable by estimating two of the
three unknowns or relating two of the unknowns to the third.   That is the crux
of the methodology adopted here and the topic of the next part.

PART III: SOIL PROPERTY ESTIMATION FOR COHESIONLESS SOILS

Relating Shear Modulus to Unit Weight

22.   An estimate of the elastic shear modulus can be obtained using the equations developed by Hardin and Richart (1963). They showed that for shearing strain amplitudes less than approximately 10^{-4}, the elastic shear modulus in clean granular materials is dependent only upon the void ratio of the soil and the ambient stress level. For materials with rounded grains, this relation is expressed by the empirical equation

$$G = \frac{2630(2.17 - e)^2}{1 + e} (\sigma_o)^{0.5} \tag{8}$$

and for soils with angular grains, it can be expressed as

$$G = \frac{1230(2.97 - e)^2}{1 + e} (\sigma_o)^{0.5} \tag{9}$$

where G is the shear modulus in psi, σ_o is the ambient stress level in psi, and e is the void ratio.

23.   The void ratio can be computed from the specific gravity G_s and dry unit weight γ_d of the soil as

$$e = \frac{G_s \gamma_w}{\gamma_d} - 1 \tag{10}$$

where $\gamma_w = 62.4$ lb/ft^3 is the unit weight of water. For most granular soils, $2.65 < G_s < 2.69$, so an average value of 2.67 should suffice. If we constrain the problem to dry soils, $\gamma_d = \gamma$ and Equation 10 reduces to

15

$$e = \frac{166.6}{\gamma} - 1 \qquad (11)$$

where γ is expressed in lb/ft^3.

Accounting for Free Surface Effects

24. The cavity expansion equations are based upon the assumption that the cavity expands in an unbounded medium. The process of cone penetration, however, takes place in a medium which is bounded above by a free surface. The existence of this free boundary allows an upward flow of the near-surface materials in the vicinity of the cone that consequently reduces the penetration resistance of the cone. This free-surface effect is especially pronounced in granular materials, but only within about 1 ft of the ground surface. Rohani and Baladi (1981) present detailed discussions of the free surface effect.

25. To account for the free-surface effect, Rohani and Baladi postulated that the shear modulus G in Equations 6 and 7 should be replaced by an apparent shear modulus G_a that varies with the penetration depth Z according to the equation:

$$G_a = 0.5 \left[A + \frac{1 - Be^{-\beta z}}{1 + Be^{-\beta z}} \right] G \qquad (12)$$

where A , B , and β are constants that reflect the cone geometry and must be evaluated experimentally. For the standard WES cone operating in cohesionless soils, A = 0.986, B = 100, and β = 0.55 in.$^{-1}$.

26. Equation 12 assumes that G is a constant. For the surficial soils of interest here, we can take G to be the shear modulus at the 12-in. depth where the free surface effects become negligible. At that depth, the hydrostatic stress σ_0 is approximately 1 psi, and Equations 8 and 9 conveniently reduce to

16

$$G = \frac{2630(2.17-e)^2}{1+e} \qquad\qquad (13)$$

and

$$G = \frac{1230(2.97-e)^2}{1+e} \qquad\qquad (14)$$

respectively. These equations uniquely relate the shear modulus to the dry unit weight of the soil (by virtue of the void ratio being uniquely determined by the dry unit weight). If we can also develop a correlation between friction angle and dry unit weight, we will have a set of three equations in three unknowns and the problem will become solvable.

Relating Friction Angle to Unit Weight

27. Many researchers have developed correlations between friction angle and dry unit weight for cohesionless soils. The majority of those correlations are, however, developed for just one or two specific soils. Consequently, they are inapplicable to the problem at hand. We require a correlation that applies to a wide range of cohesionless soil types, even if it has less accuracy than the soil-specific correlations available in the literature.

28. Figure 3 is taken from the Naval Facilities Engineering Command Design Manual 7.01 (NAVFAC 1986). It depicts approximate correlations between friction angle and dry unit weight for each of the cohesionless soil types in the USCS. This is the missing piece of the puzzle. With this chart, we now have a tractable system of three equations (CI as a function of G , ϕ , and γ_d ; G as a function of γ_d ; and ϕ as a function of γ_d) with which we can compute the three unknown engineering properties of friction angle, shear modulus, and unit weight using only CI measurements and the USCS classification.
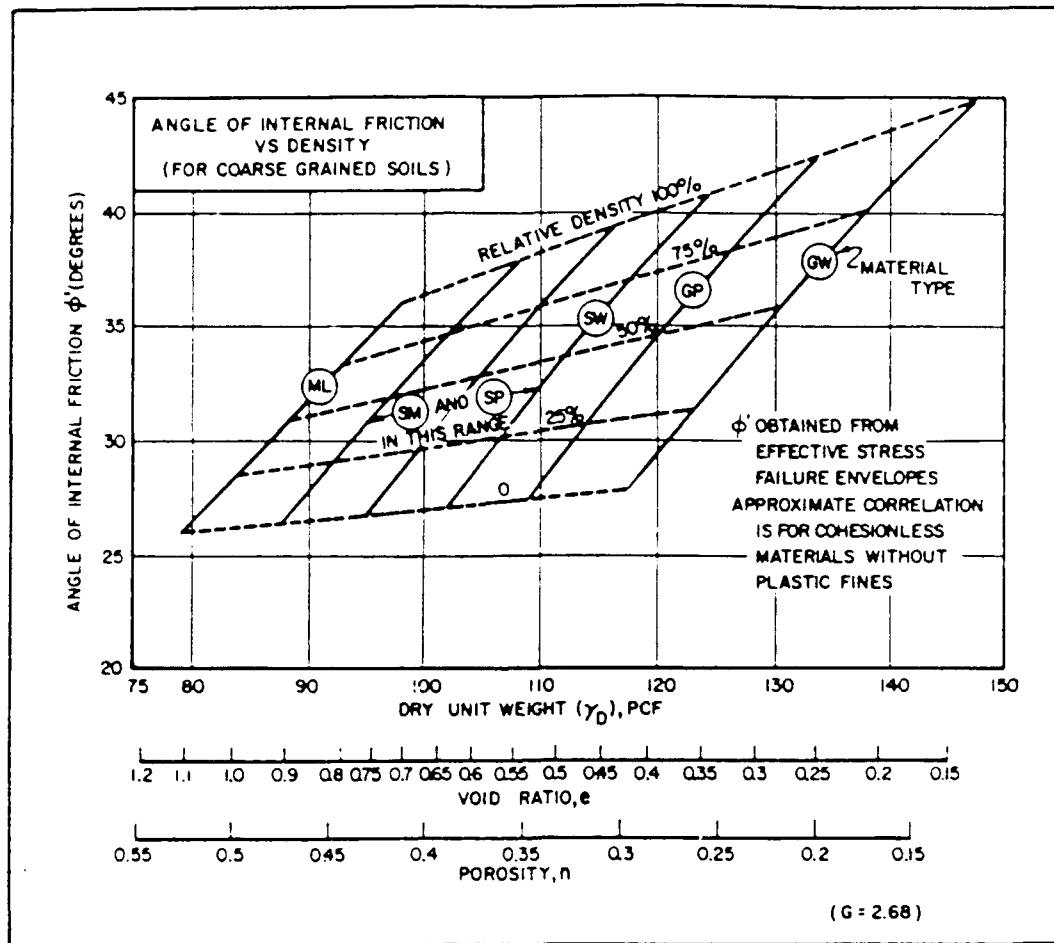
Figure 3. Strength correlations for granular soils
(Source: NAVFAC 1986 pg. 7.1-149)

Estimating The Properties of a Given Soil

29. Because the three equations discussed above are nonlinear, a closed form solution for the system of equations does not exist. Instead, a numerical solution procedure will have to be adopted. A simple trial-and-error procedure can be described as follows:

    <u>a</u>. Assume a relative density and establish corresponding values of ϕ and γ_d from the appropriate curve in Figure 3.

    <u>b</u>. Compute a void ratio e corresponding to γ_d using Equation 11.

    <u>c</u>. Compute a shear modulus G from e using either Equation 13 or Equation 14 (depending on the angularity of the grains).

18

<u>d</u>. Using the depth Z of the CI measurement, adjust G for free surface effects using Equation 12.

<u>e</u>. Substitute ϕ , γ_d , G_a , and Z into Equation 7 to obtain the theoretical value of CI.

<u>f</u>. If the measured CI exceeds the theoretical CI, choose a higher relative density; otherwise, choose a lower relative density.

<u>g</u>. Repeat the calculations until the theoretical and measured CI values agree to within a suitable tolerance.

The values of ϕ , γ_d , and G that produce a theoretical CI equal to the measured CI are the fundamental soil properties being sought.

30. The procedure above should always converge on a solution because all of the equations involved are monotonic. The number of iterations required for convergence will, of course, depend on the manner in which the iterations are performed. Since CI increases smoothly with increasing relative density (in fact, the theoretical CI is very nearly a linear function of the logarithm of relative density), a simple binary iteration approach will suffice.

31. Appendix C contains a FORTRAN subroutine implementing the procedure described above. The subroutine uses binary iteration to converge on the CI to within one percent. To prevent convergence on totally unrealistic relative densities, the search for a solution starts at a relative density of -25 percent and ends at a relative density of 150 percent. It would admittedly be rare to find soils at relative densities significantly above 100 percent (although it would certainly be possible to find soils at 105 to 110 percent). This wide range of relative densities allows for soils that are more dense in nature than they can be made using standard laboratory procedures. It also provides some leeway for soils that do not match the NAVFAC chart exactly. If a solution cannot be found within the range -25 percent < D_r < 150 percent, the subroutine is exited via an alternate return.

32. Figure 3 has been implemented in the subroutine as a tabulation of friction angle and dry unit weight values for each intersection point in the chart. These values are given in Tables 1 and 2, respectively. Simple linear interpolation within these tables is used to approximate the original curves. In order to have a single, unique relationship for each soil type, it was assumed *a priori* that SP soils will fall to the left of SM soils in the

19

Table 1. Friction angle versus relative density.

USCS Soil Type	Relative Density (%)				
	0	25	50	75	100
ML	25.9	28.4	31.1	33.4	36.0
SP	26.4	29.1	31.9	34.7	37.8
SM	26.9	29.7	32.9	35.9	39.1
SW	27.1	30.1	33.6	37.0	40.7
GP	27.5	30.7	34.6	38.3	42.5
GW	27.9	31.4	36.0	40.1	45.0

Table 2. Dry unit weight versus relative density.

USCS Soil Type	Relative Density (%)				
	0	25	50	75	100
ML	79.3	83.9	88.4	92.9	97.9
SP	87.4	92.1	97.1	102.3	107.7
SM	95.0	99.6	105.0	110.0	116.0
SW	102.1	106.4	112.1	117.7	124.3
GP	109.0	114.0	120.0	126.6	133.7
GW	117.7	123.3	130.6	138.1	147.7

figure. Thus, the order of the curves in Figure 3 is assumed to be: ML, SP,
SM, SW, GP, GW.

33. Because the shape of the soil grains will seldom be known (in many
cases, the soil type may not even be known and will have to be assumed), the
subroutine chooses between the two shear modulus equations based on the com-
puted void ratio. Hardin and Richart (1963) limit their formula for rounded
grains to void ratios less than 0.8 and imply that their formula for angular
grains only applies at void ratios of 0.6 or greater. This is based as much
on the range of their empirical data as anything; however, because soils with
rounded grains will not pack as tightly as those with angular grains for a
given relative density, it may be assumed that soils with low void ratios more
than likely have rounded grains, and those with high void ratios more than
likely have angular grains. This is exemplified by Figure 4, which shows
minimum and maximum void ratios for two materials with rounded grains and two
with angular grains. Based on these distinctions, a single, unique relation-
ship between shear modulus and void ratio was obtained by using the formula
for rounded grains at void ratios below 0.6, the formula for angular grains at
void ratios above 0.8, and a weighted average of the two for void ratios in
between.

A Caveat for Gravel Soils

34. Figure 5 shows an idealization of a MCP penetrating a gravelly
soil. In order for the cone tip to advance, the individual gravel particles
must either fail in shear or be pushed out of the way. Since the MCP is hand
operated, the loads are insufficient to fail the gravel particles; thus, par-
ticle rearrangement must control the penetration process. If individual
gravel particles are being pushed out of the way or rotated into more compact
orientations, the continuum representation implied in the cavity expansion
theory is, strictly speaking, invalid. Great care must therefore be used in
interpreting MCPT results in GP and GW soils using this methodology. The
further the soil deviates from the continuum assumptions, the greater the
potential error in the soil property estimates. This means that a well-graded
gravel with a one-half in. maximum particle size is probably amenable to
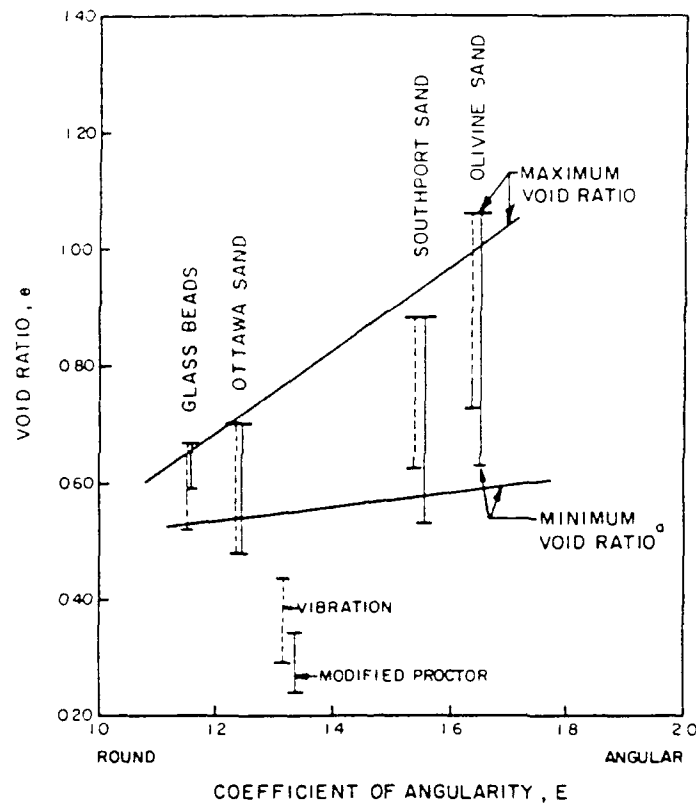
21

Figure 4. Effect of particle shape on void ratio
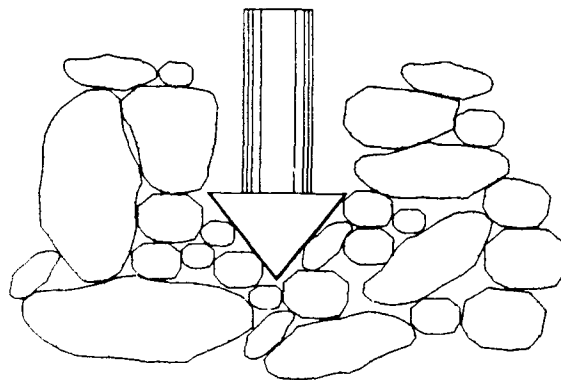(Source: Holubec and D'Appolonia 1972 pg. 308)

Figure 5. The MCPT in gravelly soils

22

interpretation using this method. On the other hand, a poorly graded gravel predominated by 2-in. particles cannot be properly analyzed.

PART IV: VALIDATION OF SOIL PROPERTY ALGORITHMS

Introduction

35.   Ideally, validation of the algorithms presented in the preceding
chapter would be accomplished using MCP, shear strength, and density tests
conducted *in situ* and in close proximity to each other. The latter require-
ment is necessary to eliminate, or at least mitigate, the problems that can
arise from areal variability in the soil properties. While *in situ* density
tests are quite common, *in situ* strength tests are seldom performed. In the
dry, cohesionless soils of interest here, an alternative would be to substi-
tute empirical relations between shear strength and dry density derived from
laboratory tests on remolded soils for the *in situ* strength tests. This can
be done as long as the MCPT and density tests are performed in carefully com-
pacted fills devoid of horizontal layering and other density variations.

36.   An extensive literature search revealed very little data that would
be suitable for validating the methodology presented in the previous chapter.
In the past, when empirical relationships based solely on CI were used for
almost all mobility modeling, there was no need to directly measure fundamen-
tal soil strength properties such as Mohr-Coulomb friction angles and cohesion
intercepts. As a result, such data were rarely collected and seldom published
(even when they were collected). Thus, the search for validation data is,
practically speaking, constrained to experimental research programs.

37.   In the research arena, there is a plethora of data available from
test programs conducted in calibration chambers. Unfortunately, those test
programs almost exclusively simulated cone penetration at depths of many t r s
of feet and stress levels far in excess of those assumed here. What little
research has been conducted in surficial soils primarily used cone penetration
resistance as the sole measure of soil strength, so there are no fundamental
strength properties to compare against.

38.   The authors managed to find a limited amount of validation data by
searching through WES reports and memoranda from the 1960's when a significant
amount of experimental research was undertaken. Unfortunately, all of the
data was obtained in two remolded sands, both classified as SP under the USCS.

24

With this in mind, the remainder of this chapter presents a very limited validation of the soil property prediction methodology.

Description of the Soils

39. Two sets of unpublished data on remolded sands were obtained from a test program conducted in the Large Blast Load Generator (LBLG) facility at WES in the mid-1960's. The materials used in those test programs were air-dry Cook's Bayou and Reid-Bedford Model sands.

40. Cook's Bayou sand is a uniform, fine sand taken from a borrow pit near Cook's Bayou in the vicinity of Vicksburg, Mississippi. The material is classified as SP according to the USCS. Its minimum and maximum dry densities are 93.3 and 110.8, respectively. Its specific gravity is 2.65, so its maximum and minimum void ratios are 0.77 and 0.49, respectively. The grain shape is subrounded.

41. Reid-Bedford Model sand (hereafter referred to simply as Reid-Bedford sand) is a uniform, fine sand obtained from a borrow pit near the Big Black River in the vicinity of Vicksburg, Mississippi. The name is derived from the hydrologic model at WES in which it was first used. The material is classified as SP under the USCS. Its minimum and maximum dry densities are 87.2 and 104.2 pcf, respectively. Its specific gravity is between 2.65 and 2.66, so its maximum and minimum void ratios are approximately 0.90 and 0.59, respectively. The grain shape is on the border line between subrounded and subangular.

42. The strength properties of both sands have been documented in WES reports by McNulty (1965) and Kennedy, Albritton, and Walker (1966). These are summarized as strength-density curves in Figures 6 and 7. Also included in those figures are least-square regression lines that are plotted over the range of densities from minimum to maximum for each soil. The regression line for the Cook's Bayou sand is given by

$$\phi = 0.693 \gamma_d - 33.6 \tag{15}$$
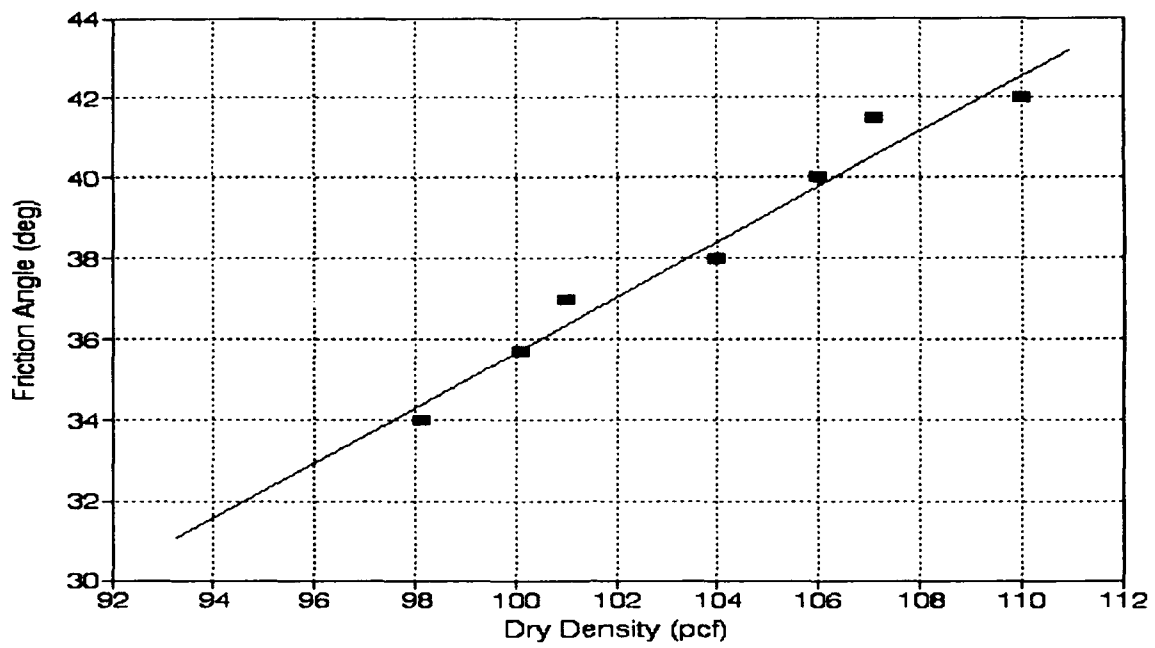
and the regression line for Reid-Bedford sand is given by

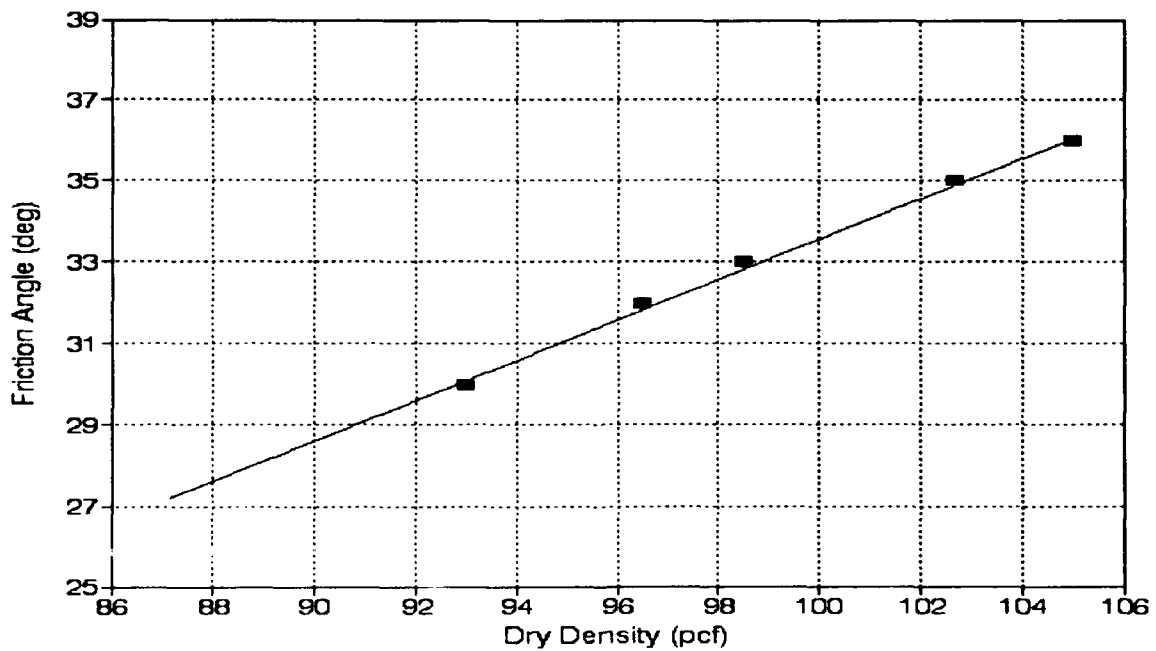Figure 6. Strength-density relationship for Cook's Bayou sand

Figure 7. Strength-density relationship for Reid-Bedford sand

26

$$\phi = 0.529 \, \gamma_d - 19.3 \qquad\qquad (16)$$

where the dry unit weight γ_d is in pcf and the friction angle ϕ is in degrees.

Validation of the Methodology

43. The purpose of the LBLG test program from which the validation data were obtained was to study the response of buried arch structures to blast loading. Six test specimens, each 23 ft in diameter and 10 ft deep, were constructed to contain the model arches. The specimens were built in 6-in. lifts using a hand-towed vibrating plate to achieve a consistent specimen density. At the completion of every other lift, a series of box-density and cone-penetration tests were conducted at various locations across the specimen surface. For validation purposes, tests conducted in close proximity to the model arches have been ignored, leaving approximately 50 CI profiles for each specimen. These CI profiles consisted of readings taken at 1-in. depth intervals for a distance of 12 in. or until the range of the micrometer dial was exceeded. For our use, the CI profiles have been tabulated at 2-in. depth intervals and an average CI profile has been obtained for each specimen by averaging the cone indices at each depth. The averaged CI profiles for the six test specimens (designated here as LBLG-1 through LBLG-6) are given in Table 3.

44. In support of the large-scale testing, four small-scale specimens were built by raining the sand into a 48-in.-diam mold. Each of these small specimens was initially built to a height of 18 in., at which point five cone penetration tests were performed. Following this, the upper 6 in. of each specimen was removed and box density tests were conducted on the top 2 in. of the remaining material. This provided dry unit weight data at approximately the mid-height of the cone profiles. Cone penetration data from only one of those specimens were available. That data have been averaged as well and is included in Table 3 as specimen LBLG-7.

45. For each specimen in Table 3, the subroutine listed in Appendix C was used to estimate a friction angle and a dry unit weight at each tabulated

Table 3. Average cone profiles for the LBLG test specimens.

Specimen Number	Soil Type	Mean Dry Unit Weight (pcf)	Cone Diameter (in.)	Cone Depth (in.)	Mean Cone Index (psi)
LBLG-1	Cook's Bayou	101.4	0.8	2	40
				4	91
				6	182
				8	275
LBLG-2	Cook's Bayou	107.0	0.5	2	58
				4	143
				6	282
				8	439
				10	521
LBLG-3	Reid-Bedford	100.5	0.5	2	27
				4	60
				6	107
				8	201
				10	280
				12	383
LBLG-4	Cook's Bayou	107.4	0.5	2	56
				4	133
				6	253
				8	397
				10	533
LBLG-5	Cook's Bayou	101.7	0.5	2	36
				4	69
				6	124
				8	226
				10	289
				12	363
LBLG-6	Reid-Bedford	106.5	0.5	2	68
				4	154
				6	290
				8	493
				10	611
LBLG-7	Cook's Bayou	107.8	0.5	2	35
				4	86
				6	152
				8	225
				10	290
				12	360

depth. The soil type and CI data input to the subroutine and the friction angle and dry unit weight estimates output from it are presented in Table 4. For each test specimen, a comparison between the soil properties measured in the LBLG (actually, the dry unit weights measured in the LBLG and friction angles computed from those data using Equations 15 and 16) and the average of the predicted soil properties are given in Table 5.

46. To better illustrate the amount of agreement, the predicted friction angles are plotted against the measured friction angles in Figure 8 and the predicted dry unit weights are plotted against the measured dry unit weights in Figure 9. Both figures show very good agreement between the predicted and the measured values. There seems to be a slight tendency towards overprediction, especially for the unit weights, but the degree of overprediction is slight.

47. The data presented here by no means constitute complete validation of the model; however, it does show the potential predictive capabilities of the methodology. Based of these results, continued work, in the form of further validation and refinement of the model, is definitely warranted.

Table 4. Soil property predictions for the LBLG specimens.

Soil Specimen	Input Data					Output Data	
	USCS Soil Class	Cone Width (in.)	Cone Depth (in.)	Number of Tests	Average CI (psi)	Dry Unit Weight (pcf)	Friction Angle (deg)
LBLG-1	SP	0.8	2	50	40	109.3	38.7
			4	50	91	107.7	37.8
			6	50	182	107.7	37.8
			8	44	275	106.1	36.9
LBLG-2	SP	0.5	2	50	58	115.9	42.5
			4	50	143	115.5	42.3
			6	50	282	115.1	42.1
			8	50	439	113.5	41.1
			10	44	521	110.7	39.5
LBLG-3	SP	0.5	2	56	27	102.3	34.7
			4	56	60	100.7	33.9
			6	56	107	99.4	33.2
			8	56	201	101.3	34.1
			10	46	280	101.3	34.1
			12	46	383	102.8	35.0
LBLG-4	SP	0.5	2	50	56	115.5	42.3
			4	50	133	114.3	41.6
			6	50	253	113.1	40.9
			8	50	397	111.7	40.1
			10	48	533	110.9	39.7
LBLG-5	SP	0.5	2	64	36	107.4	37.6
			4	64	69	102.8	35.0
			6	64	124	101.5	34.3
			8	64	226	102.8	35.0
			10	64	289	101.5	34.3
			12	59	363	102.0	34.6
LBLG-6	SP	0.5	2	26	68	-	-
			4	26	154	116.7	43.0
			6	26	290	115.5	42.3
			8	26	493	115.5	42.3
			10	18	611	113.1	40.9
LBLG-7	SP	0.5	2	20	35	106.9	37.3
			4	20	86	106.6	37.2
			6	20	152	104.5	35.9
			8	20	225	102.8	35.0
			10	20	290	101.5	34.3
			12	20	360	102.0	34.6

Table 5. Comparison of predicted and measured values.

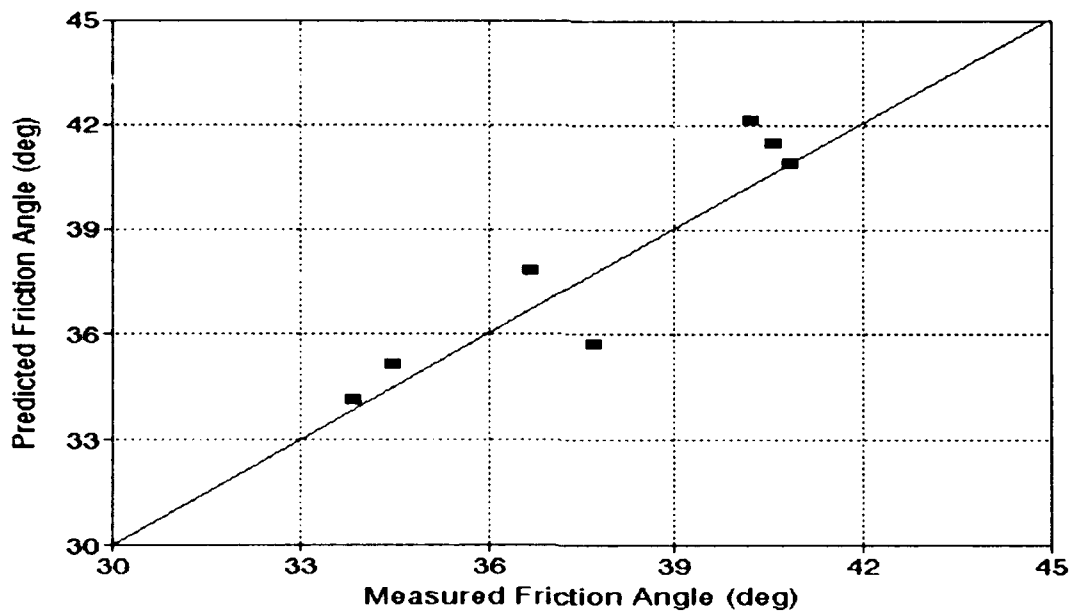| Soil Specimen	Soil Type	Dry Unit Weight (pcf)		Friction Angle (deg)	
		Measured	Predicted	Measured	Predicted
LBLG-1	Cook's Bayou	101.4	107.7	36.7	37.8
LBLG-2	Cook's Bayou	107.0	114.1	40.6	41.5
LBLG-3	Reid-Bedford	100.5	101.3	33.8	34.2
LBLG-4	Cook's Bayou	107.4	113.1	40.8	40.9
LBLG-5	Cook's Bayou	101.7	103.0	34.5	35.1
LBLG-6	Reid-Bedford	106.5	115.2	40.2	42.1
LBLG-7	Cook's Bayou	107.8	104.1	37.7	35.7

Figure 8. Predicted friction angle versus measured friction angle
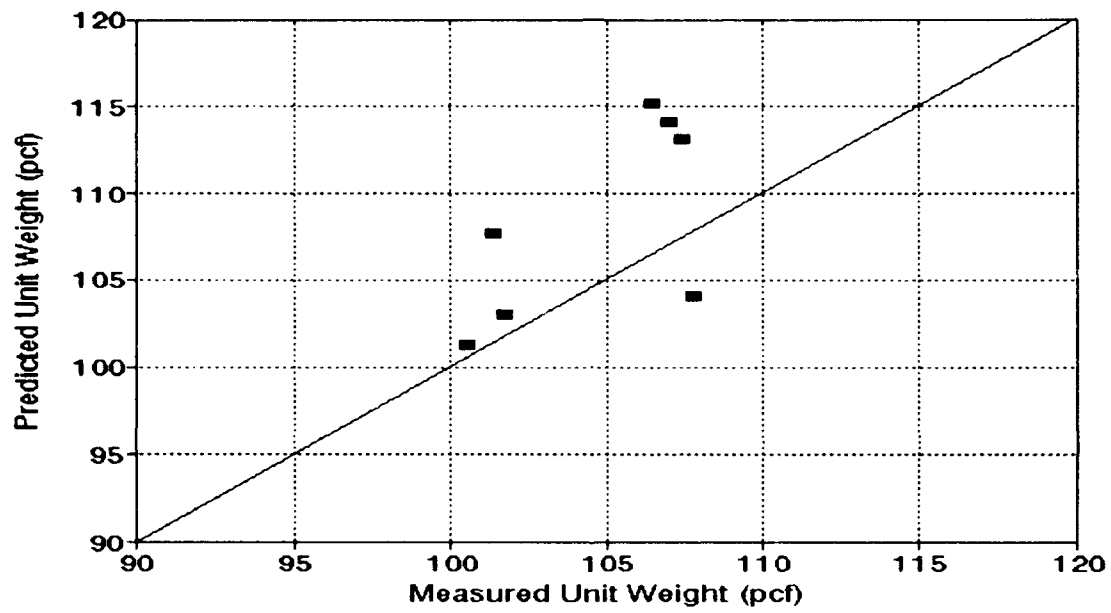
31

Figure 9.   Predicted dry unit weight versus measured
dry unit weight

PART V: SUMMARY, CONCLUSIONS, AND RECOMMENDATIONS

Summary

48.   A methodology has been presented for estimating the fundamental
engineering properties of cohesionless soils from data collected with the MCP.
The theoretical approach couples static force equilibrium with cavity expan-
sion theory to model the response of the soil to penetration by a cone tip.
The mathematical description of the cone penetration process is augmented by
several empirical relationships that serve to reduce the number of unknowns
and make the problem tractable.   Limited validation using unpublished data
collected in two SP soils shows that the technique can provide reasonable
estimates of total unit weight and Mohr-Coulomb friction angle.   This partial
validation suggests that the methodology warrants further development.

Conclusions and Recommendations

49.   Additional validation data are needed before this method can be
used without reservation.   Continued literature searches and additional labo-
ratory and field experimentation are needed to further validate and refine the
methodology. In order to be usable, validation data must include *in situ* mea-
surements of unit weight, shear strength, shear stiffness, and cone penetra-
tion resistance--all taken in close proximity to one another.

50.   Future research should be directed towards refining the existing
methodology for cohesionless soils and extending the theory to cohesive soils.
It is hoped that, eventually, a system can be devised that is applicable in
all soil types.   One approach would be to collect several methodologies such
as the one described here and embed them within a knowledge-based-system
(KBS).   A KBS (which includes, but is not limited to, so-called "expert sys-
tems") is a computer program that combines knowledge about a specific domain
and reasoning abilities to arrive at conclusions.   In the domain of soil-
property estimation, a KBS might combine cone penetration and soil description
data supplied by the user with a collection of theoretical and empirical
models to arrive at estimates of the soil properties.   The KBS would choose
the appropriate model(s), infer or ask for any missing data, and sort out the

often conflicting answers that the models produce. The research described here is a first step towards producing such a system.

REFERENCES

Baldi, G., Bellotti, R., Ghionna, V., Jamiolkowski, M., and Pasqualini, E. 1981. "Cone Resistance of a Dry Medium Sand," *Proceedings, 10th International Conference on Soil Mechanics and Foundation Engineering*, Stockholm, Vol 2, pp 427-432.

Baligh, M. M. 1976. "Cavity Expansion in Sand with Curved Envelopes," *Journal of the Geotechnical Engineering Division*, ASCE, Vol 102, No. GT11, pp 1131-1146.

Farr, J. V. 1991. "Shear Strength Properties From Cone Index Tests," *Proceedings, 5th European Conference of the International Society of Vehicle Terrain Interaction*, Budapest, Hungary.

Greeuw, G., Smits, F. P., and van Driel, P. 1988. "Cone Penetration Tests in Dry Oosterschelde Sand and the Relation with a Cavity Expansion Model," *Penetration Testing 1988*, pp 771-776.

Hardin, B. O., and Richart, F. E., Jr. 1963. "Elastic Wave Velocities in Granular Soils," *Journal of the Soil Mechanics and Foundation Engineering Division*, ASCE, Vol 92, No. SM2, pp 27-42.

Holubec, I., and D'Appolonia, E. 1973. "Effect of Particle Shape on the Engineering Properties of Granular Soils," *Evaluation of Relative Density and Its Role in Geotechnical Projects Involving Cohesionless Soils*, STP 523, ASTM, pp. 304-318.

Karafiath, L. L., and Nowatzki, E. A. 1978. *Soil Mechanics in Off-Road Vehicle Engineering*, Trans Tech Publications, Bay Village, OH, pp 254-263.

Kennedy, T. E., Albritton, G. E., and Walker, R. E. 1966. "Initial Evaluation of the Free-Field Response of the Large Blast Load Generator," Technical Report 1-723, US Army Engineer Waterways Experiment Station, Vicksburg, MS.

McNulty, J. W. 1965. "An Experimental Study of Arching in Sand," Technical Report 1-674, US Army Engineer Waterways Experiment Station, Vicksburg, MS.

Meier, R. W., and Baladi, G. Y. 1988. "Cone-Index-Based Estimates of Soil Strength: Theory and User's Guide For Computer Code CIBESS," Technical Report SL-88-11, US Army Engineer Waterways Experiment Station, Vicksburg, MS.

NAVFAC. 1986. *Soil Mechanics*, Design Manual 7.01, Naval Facilities Engineering Command, Alexandria, VA.

Robertson, P. K., and Campanella, R. G. 1983. "Interpretation of Cone Penetration Tests. Part I: Sand," *Canadian Geotechnical Journal*, Vol 20, pp 718-733.

Rohani, B., and Baladi, G. Y. 1981. "Correlation of Mobility Cone Index with Fundamental Engineering Properties of Soil," Technical Report SL-81-4, US Army Engineer Waterways Experiment Station, Vicksburg, MS.

Rula, A. A., and Nuttall, C. J., Jr. 1971. "An Analysis of Ground Mobility Models (ANAMOB)," Technical Report M-71-4, US Army Engineer Waterways Experiment Station, Vicksburg, MS.

Vesić, A. S. 1963. "Bearing Capacity of Deep Foundations in Sand," *Stresses in the Soil and Layered Systems*, Record 39, Highway Research Board, Washington, DC, pp 112-153.

Vesić, A. S. 1972. "Expansion of Cavities in Infinite Soil Masses," *Journal of the Soil Mechanics and Foundation Division*, ASCE, Vol 98, No. SM3, pp 265-290.

Vesić, A. S. 1977. *Design of Pile Foundations*, NCHRP Synthesis of Highway Practice No. 42, Transportation Research Board, Washington, DC.

APPENDIX A: UNIFIED SOIL CLASSIFICATION SYSTEM

Table A1

Detailed description of the USCS soil classes

USCS Soil Classification	Description
GW	Well graded gravels, gravel-sand mixtures, little or no fines, wide range of grain sizes
GP	Poorly graded gravels, gravel-sand mixtures, little or no fines, narrow range of grain sizes
GM	Silty gravels, poorly graded gravel-sand-silt mixtures, nonplastic fines or fines with little plasticity
GC	Clayey gravels, poorly graded gravel-sand-clay mixtures, plastic fines
SW	Well graded sands, gravelly sands, little or no fines, wide range of grain sizes
SP	Poorly graded sands, gravelly sands, little or no fines, narrow range of grain sizes
SM	Silty sands, poorly graded sand-silt mixtures, nonplastic fines or fines with low plasticity
SC	Clayey sands, poorly graded sand-clay mixtures, plastic fines
ML	Inorganic silts and very fine sands, rock flour, silty or clayey fine sands with slight plasticity
CL	Inorganic clays of low to medium plasticity, gravelly clays, sandy clays, silty clays, lean clays
OL	Organic silts and organic silty-clays of low plasticity
MH	Inorganic silts, micaceous or diatomaceous fine sandy or silty soils, elastic silts
CH	Inorganic clays of high plasticity, fat clays
OH	Organic clays of medium to high plasticity
PT	Peat and other highly organic soils

APPENDIX B: DERIVATION OF THE CAVITY EXPANSION EQUATIONS

1. The problem of the quasi-static expansion of a spherical cavity in an unbounded, compressible, elastic-plastic medium obeying the Mohr-Coulomb failure criterion was first solved by Vesić (1972).* His solution is summarized here for the convenience of the reader.

2. The objective is to determine the radial stress σ_p at the cavity surface necessary to maintain a slow expansion of the cavity. Referring to Figure B1, stress equilibrium for an element located at some distance r from the center of the cavity can be written as

$$\frac{\partial \sigma_r}{\partial r} + 2 \frac{\sigma_r - \sigma_\theta}{r} = 0 \tag{B1}$$

where σ_r is the radial stress and σ_θ is the circumferential stress. If it is assumed that the material immediately beyond the cavity is in a state of incipient failure (i.e., limit equilibrium is invoked), then the radial and circumferential stresses can be related through the failure criterion as

$$\sigma_r - \sigma_\theta = (\sigma_r + \sigma_\theta)\sin\phi + 2\,c\,\cos\phi \tag{B2}$$

where c is the Mohr-Coulomb cohesion intercept and ϕ is the Mohr-Coulomb friction angle. Combining Equations B1 and B2, the governing differential equation for the radial stresses around the cavity becomes

$$\frac{\partial \sigma_r}{\partial r} + \frac{4}{r}\left(\frac{\sin\phi + 2\,c\,\cos\phi}{1 + \sin\phi}\right) = 0 \tag{B3}$$

This equation must be solved subject to the boundary conditions shown in the figure.

3. Equation B3 is a first-order differential equation of the form

---

* References cited in this appendix are listed in the References section at the end of the main text.

B3
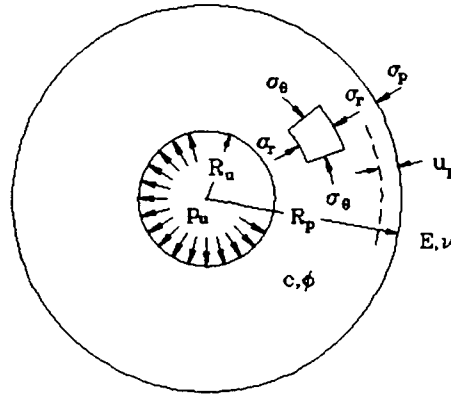
Figure B1. Expansion of a spherical
cavity (after Vesic 1972)

$$\frac{dy}{dx} + P(x) \cdot y = Q(x) \tag{B4}$$

where

$$y \equiv \sigma_r$$

$$dx \equiv dr$$

$$P(x) = \frac{4}{r} \left(\frac{\sin \phi}{1 + \sin \phi} \right)$$

$$Q(x) = \frac{4}{r} \left(\frac{c \cos \phi}{1 + \sin \phi} \right)$$

Its solution is given by

$$y = C_1 \, e^{-\int P(x)\,dx} + e^{-\int P(x)\,dx} \int e^{-\int P(x)\,dx} \cdot Q(x) \; dx \tag{B5}$$

B4

where C_1 is an integration constant. Applying the boundary condition $\sigma_r = p_u$ at $r = R_u$ and completing the integration:

$$\sigma_r = (P_u + c \cot\phi)\left(\frac{R_u}{r}\right)^{\frac{4\sin\phi}{1+\sin\phi}} - c \cot\phi \tag{B6}$$

This expression relates the radial stresses in the vicinity of the cavity to the instantaneous size of the cavity and the internal cavity pressure.

4.   To determine the pressure p_u needed to expand the cavity to some radius R_u, Vesić first applied the continuity condition that the change in volume of the cavity must be equal to the change in volume of the elastic zone plus the change in volume of the plastic zone:

$$R_u^3 = R_p^3 - (R_p - u_p)^3 + (R_p^3 - R_u^3)\Delta \tag{B7}$$

where u_p is the radial displacement of the boundary between the elastic and plastic zones, Δ is the average volumetric strain in the plastic zone, and it is assumed that the initial cavity radius is zero.   From elastic theory, the displacement of the elastic/plastic boundary is proportional to the increase in radial stress above the initial ambient pressure q :

$$u_p = \frac{1}{4G}(\sigma_p - q)R_p \tag{B8}$$

Substituting Equation B8 into Equation B7 and ignoring higher powers of u_p :

$$1 + \Delta = \frac{R_p^3}{R_u^3}\left[\frac{3}{4G}(\sigma_p - q) + \Delta\right] \tag{B9}$$

Substituting $r = R_p$ in Equation B6 provides an expression for σ_p :

B5

$$\sigma_p = (p_u + c \cot \phi) \left(\frac{R_u}{R_p} \right)^{\frac{4 \sin \phi}{1 + \sin \phi}} - c \cot \phi \tag{B10}$$

Stress equilibrium requires that

$$(p_u + c \cot \phi) \left(\frac{R_u}{R_p} \right)^{\frac{4 \sin \phi}{1 + \sin \phi}} - c \cot \phi \tag{B11}$$

Substituting Equations B10 and B11 into Equation B9, the following expression for the ratio of the plastic zone radius to the cavity radius is obtained:

$$\sqrt[3]{1 + \Delta} = \frac{R_p}{R_u} \sqrt[3]{\left(\frac{c + q \tan \phi}{G} \right) \left(\frac{3 \cos \phi}{3 - \sin \phi} \right) + \Delta} \tag{B12}$$

Noting that for Δ small

$$\sqrt[3]{1 + \Delta} \approx 1$$

and for $\phi < 45°$

$$\frac{3 \cos \phi}{3 - \sin \phi} \approx 1$$

Equation B12 can be simplified and rearranged to produce the approximation

$$\frac{R_p}{R_u} = \sqrt[3]{\frac{I_r}{1 + I_r \Delta}} \tag{B13}$$

in which I_r , the rigidity index, is equal to the ratio of the shear modulus of the soil to its initial strength:

B6

$$I_r = \frac{G}{c + q \tan\phi}$$

5. If the material is assumed to be incompressible (i.e., $\Delta = 0$), Equation B13 reduces to

$$\frac{R_p}{R_u} = \sqrt[3]{I_r} = \left(\frac{G}{c + q \tan\phi}\right)^{\frac{1}{3}} \tag{B14}$$

Substituting this equation back into Equation B10, we arrive at the required expression for the stress at the cavity surface (i.e., at $r = R_u$):

$$\sigma_p = 3 \left(q + c \cot\phi \right) \left(\frac{1 + \sin\phi}{3 - \sin\phi}\right) I_r^{\frac{4 \sin\phi}{3(1 - \sin\phi)}} - c \cot\phi \tag{B15}$$

This is used in Chapter 2 to derive an expression for the normal stresses acting on the cone surface.

B7

APPENDIX C: A FORTRAN IMPLEMENTATION OF THE METHODOLOGY

```
C     ===================================================================
C              Binary Iteration Routine for Solving Cone Index Equation
C     ===================================================================
C
C                              INPUT VARIABLES
C
C     Width    - Maximum cone diameter in inches (real)
C     USCS     - USCS soil classification (2-character string)
C     Z        - Cone index measurement depth in inches (real)
C     CI       - Measured cone index in psi (real)
C
C                              OUTPUT VARIABLES
C
C     Density - Relative density in percent (real)
C     Gamma   - Dry unit weight in pcf (real)
C     Phi     - Friction angle in degrees (real)
C     G       - Elastic shear modulus in psi (real)
C     *       - Alternate return for error condition
C
C                              LOCAL VARIABLES
C
C     Soil    - Soil type index into Angles and Gammas arrays (integer)
C     Lower   - Density index into Angles and Gammas arrays (integer)
C     Angles  - Array of friction angles for each soil type (real)
C     Gammas  - Array of unit weights for each soil type (real)
C     Symbol  - Array of USCS soil classification symbols (character*2)
C     E       - Void ratio (real)
C     AngleG  - Shear modulus for angular soils in psi (real)
C     RoundG  - Shear modulus for rounded soils in psi (real)
C     Predict - Computed cone index in psi (real)
C
C     -------------------------------------------------------------------

      Subroutine SOLVER (USCS,Z,CI,Density,Gamma,Phi,G,*)

      Integer Soil,Lower
      Real Angles(5,6),Gammas(5,6)
      Real Width,Z,CI,Phi,G,Gamma,E,Density
      Real Increment,Ratio,Delta,Fuzz,AngleG,RoundG,Predict
      Character USCS*2,Symbol*2(2,6)

      Data Symbol / 'gw' , 'GW' ,
     1              'gp' , 'GP' ,
     2              'sw' , 'SW' ,
     3              'sm' , 'SM' ,
     4              'sp' , 'SP' ,
     5              'ml' , 'ML' /

      Data Angles / 27.9 , 31.4 , 36.0 , 40.1 , 45.0 ,
     1              27.5 , 30.7 , 34.6 , 38.3 , 42.5 ,
     2              27.1 , 30.1 , 33.6 , 37.0 , 40.7 ,
     3              26.9 , 29.7 , 32.9 , 35.9 , 39.1 ,
     4              26.4 , 29.1 , 31.9 , 34.7 , 37.8 ,
     5              25.9 , 28.4 , 31.1 , 33.4 , 36.0 /

      Data Gammas /117.7 ,123.3 ,130.6 ,138.1 ,147.7 ,
     1             109.0 ,114.0 ,120.0 ,126.6 ,133.7 ,
```

```
      2                   102.1 ,106.4 ,112.1 ,117.7 ,124.3 ,
      3                    95.0 , 99.6 ,105.0 ,110.0 ,116.0 ,
      4                    87.4 , 92.1 , 97.1 ,102.3 ,107.7 ,
      5                    79.3 , 83.9 , 88.4 , 92.9 , 97.9 /

C ... convert soil classification symbol to an array index

      Do 1 J=1,6
      Do 1 I=1,2
    1 If (USCS.EQ.Symbol(I,J)) Soil = J

C ... initialize relative density and zero tolerance for convergence

      Density = -25.0
      Increment = 25.0
      Fuzz = 0.01*CI

C ... convert relative density guess to an array index

    2 Lower = MAX( 0 , MIN ( INT(Density/25) , 3 ))

C ... use linear interpolation to compute phi and gamma from density

      Ratio = (Density-25*Lower)/25

      Delta = Angles(Lower+2,Soil) - Angles(Lower+1,Soil)
      Phi   = Angles(Lower+1,Soil) + Delta*Ratio

      Delta = Gammas(Lower+2,Soil) - Gammas(Lower+1,Soil)
      Gamma = Gammas(Lower+1,Soil) + Delta*Ratio

C ... compute void ratio from gamma and shear modulus from void ratio

      E = (2.68 * 62.4 / Gamma) - 1.0

      If (E.LE.0.6) Then
         G = 2630 * (2.17-E)**2 / (1.0+E)
      Else If (E.GE.0.8) Then
         G = 1230 * (2.97-E)**2 / (1.0+E)
      Else
         RoundG = 2630 * (2.17-E)**2 / (1.0+E)
         AngleG = 1230 * (2.97-E)**2 / (1.0+E)
         G = (E-0.6)/0.2*RoundG + (0.8-E)/0.2*AngleG
      End If

C ... compute cone index corresponding to phi, g, gamma, and depth

      Predict = CONE(Phi,G,Gamma,Z,Width)

C ... compare to measured cone index and adjust density guess as needed

      If (ABS(Predict-CI).LT.Fuzz) RETURN
      If (Predict.GT.CI) Then
         If (Density.LE.-25.0) Then
            RETURN 1
         Else
            Increment = 0.5*Increment
```

```
            Density - Density - Increment
        End If
    Else
        If (Density.GE.150.0) Then
            RETURN 1
        Else
            Density = Density + Increment
        End If
    End If

C ... compute another cone index estimate using the new relative density

    Go To 2

    End
```

```
C       ■■■■■■■■■■■■■■■■■■■■■■■■■■■■■■■■■■■■■■■■■■■■■■■■■■■■■■■■■■■■■■■■■■■■
C                   Mathematical Model for Computing Cone Index
C       ■■■■■■■■■■■■■■■■■■■■■■■■■■■■■■■■■■■■■■■■■■■■■■■■■■■■■■■■■■■■■■■■■■
C
C                                    INPUT
C
C       Phi      - Friction angle in degrees (real)
C       G        - Elastic shear modulus in psi (real)
C       Gamma    - Dry unit weight in pcf (real)
C       Z        - Cone index measurement depth in inches (real)
C       Width    - Maximum cone diameter in inches (real)
C
C       -----------------------------------------------------------------
C

        Function CONE(Phi,G,Gamma,Z,Width)

        Parameter (Alpha=15.0,A=0.986,B=100.0,Beta=0.55)

        Double Precision GammaTanPhi,Term1,Term2,Omega
        Real Phi,G,Gamma,Z,Pi,TanAlpha,SinPhi,TanPhi,H,M,Ga

C ... compute cone height from width and apex angle

        Pi = ATAN2(0.0,-1.0)
        TanAlpha = TAN(Pi*Alpha/180)
        H = 0.5*Width/TanAlpha

C ... compute trig functions involving friction angle

        SinPhi = SIN(Pi*Phi/180)
        TanPhi = TAN(Pi*Phi/180)
        GammaTanPhi = (Gamma/1728)*TanPhi

C ... compute the exponent of the shear modulus

        M = 4./3. * SinPhi/(1.+SinPhi)

C ... compute the omega term

        Term1 = ((Z+H)*GammaTanPhi)**(3-M)
        Term2 = (Z+(3-M)*H) * GammaTanPhi * (Z*GammaTanPhi)**(2-M)
        Omega = (Term1-Term2) / (2-M) / (3-M) / (H*GammaTanPhi)**2

C ... adjust the shear modulus for free surface effects

        Ga = 0.5 * G * (A + (1.-B*EXP(-Beta*Z)) / (1.+B*EXP(-Beta*Z)) )

C ... compute and return the cone index

        CONE = 6 * Ga**M * Omega
       1          * (1.+SinPhi) / (3.-SinPhi)
       2          * (TanAlpha+TanPhi) / (TanAlpha*TanPhi)

        Return
        End
```

APPENDIX D: NOTATION

A	Empirical constant used to calculate apparent shear modulus
B	Empirical constant used to calculate apparent shear modulus
c	Mohr-Coulomb cohesion intercept
C_1	Constant of integration
CI	Cone index (cone penetration resistance)
D_r	Relative density of the soil
E	Coefficient of angularity of the soil grains
e	Void ratio of the soil
F_z	Measured vertical force on the cone
G	Initial elastic shear modulus of the soil
G_a	Apparent shear modulus (adjusted for free-surface effects)
G_s	Specific gravity of the soil
I_r	Rigidity index of the soil
L	Length of the cone tip
m	Shear modulus exponent in the cone index equation
n	Porosity of the soil
P_u	Pressure inside a spherical cavity of arbitrary radius
q	Overburden stress at an arbitrary depth
r	Arbitrary radius of the cone tip
R_u	Arbitrary radius of an expanding spherical cavity
R_p	Arbitrary radius of the plastic zone around the cavity
u_p	Arbitrary displacement of the elastic-plastic boundary
Z	Depth of cone penetration
α	Apex angle of the cone tip
β	Empirical constant used to calculate apparent shear modulus
Δ	Volumetric strain in the vicinity of the cavity
γ	Total unit weight of the soil
γ_d	Dry unit weight of the soil
γ_w	Unit weight of water
η	Arbitrary vertical distance from the cone tip
σ	Arbitrary normal stress acting on the cone tip
σ_o	*In situ* confining pressure
σ_p	Pressure inside an expanding spherical cavity
σ_r	Arbitrary radial stress
σ_θ	Arbitrary circumferential stress

τ	Arbitrary shear stress acting on the cone tip
ϕ	Mohr-Coulomb friction angle
Ω	Term used to simplify the cone index equation